

# Resonant soft x-ray magnetic scattering from the 4*f* and 3*d* electrons in DyFe<sub>4</sub>Al<sub>8</sub>: Magnetic interactions in a cycloidal antiferromagnet

T. A. W. Beale,<sup>1</sup> S. B. Wilkins,<sup>2</sup> P. D. Hatton,<sup>1,\*</sup> P. Abbamonte,<sup>3</sup> S. Stanescu,<sup>4,†</sup> and J. A. Paixão<sup>5</sup>

<sup>1</sup>*Department of Physics, University of Durham, Rochester Building, South Road, Durham, DH1 3LE, United Kingdom*

<sup>2</sup>*Condensed Matter Physics & Materials Science Department, Brookhaven National Laboratory, Upton, New York, 11973-5000, USA*

<sup>3</sup>*Frederick Seitz Materials Research Laboratory, Department of Physics, University of Illinois, 1110 West Green Street, Urbana, Illinois 61801-3080, USA*

<sup>4</sup>*European Synchrotron Radiation Facility, Boîte Postal 220, F-38043 Grenoble Cedex, France*

<sup>5</sup>*Departamento de Física, University of Coimbra, P-3000 Coimbra, Portugal*

(Received 19 December 2006; revised manuscript received 21 March 2007; published 22 May 2007)

Soft x-ray resonant scattering has been used to examine the charge and magnetic interactions in the cycloidal antiferromagnetic compound DyFe<sub>4</sub>Al<sub>8</sub>. By tuning to the Dy *M*<sub>4</sub> and *M*<sub>5</sub> absorption edges and the Fe *L*<sub>2</sub> and *L*<sub>3</sub> absorption edges, we can directly observe the behavior of the Dy 4*f* and Fe 3*d* electron shells. Magnetic satellites surrounding the (110) Bragg peak were observed below 65 K. The diffraction peaks display complex spectra at the Dy *M*<sub>5</sub> edge, indicative of a split 4*f* electron band. This is in contrast to the simple resonance observed at the Fe *L*<sub>3</sub> absorption edge, which probes the Fe 3*d* electron shell. Temperature-dependent measurements detail the ordering of the magnetic moments on both the iron and the dysprosium antiferromagnetic cycloids. The ratio between the superlattice peak intensities of the Dy *M*<sub>4</sub> and *M*<sub>5</sub> absorption edges remained constant throughout the temperature range, in contrast to a previous study conducted at the Dy *L*<sub>2,3</sub> edges. Our results demonstrate the ability of soft x-ray diffraction to separate the individual magnetic components in complicated multielement magnetic structures.

DOI: 10.1103/PhysRevB.75.174432

PACS number(s): 75.25.+z, 61.10.-i, 71.20.Eh, 75.47.Np

## I. INTRODUCTION

The combination of both rare earth and transition metal elements within a single compound raises interesting possibilities for studying their magnetic interactions.<sup>1–6</sup> Deciphering the individual magnetic contributions within these compounds is essential to obtain an overall understanding of the bulk properties of the sample. The series of compounds *R*Fe<sub>4</sub>Al<sub>8</sub>, where *R* is a rare earth or actinide element, show unusual magnetic properties;<sup>7–9</sup> their highly symmetric structure and the relatively weak interaction between the two magnetic lattices in the compound provides an ideal platform for studying the interplay between the magnetic ions. As such, the combined contribution from both the iron and the rare earth ions to the overall magnetic structure of DyFe<sub>4</sub>Al<sub>8</sub> has stimulated considerable interest.<sup>10–13</sup> In addition, compounds with a higher iron content, such as SmFe<sub>10</sub>Si<sub>2</sub>,<sup>14</sup> are ferromagnets with a high Curie temperature and have a relatively large magnetic anisotropy, factors that are technologically important for high-field magnets.

The title compound forms a body centered unit cell with space group<sup>15</sup> *I4/mmm* (*a*=*b*=8.731 Å, *c*=5.005), where the dysprosium atoms occupy the eight corners and the central position at the unit cell (Fig. 1). Iron atoms occupy a further eight sites forming a cuboid around each dysprosium atom, and the aluminum atoms occupy the remaining positions. Detailed studies using neutron diffraction<sup>16</sup> and x-ray magnetic scattering at the Dy *L*<sub>2,3</sub> edges<sup>17</sup> proposed a complicated magnetic structure, where at low temperatures both the dysprosium and iron magnetic moments are ordered into a cycloidal structure. Below *T*<sub>N</sub> the iron orders antiferromagnetically in the [110] direction, with a small, long-wavelength, modulation superimposed resulting in a cyclic rotation of the moments in the *ab* plane with a period of

approximately 15 unit cells. At a lower temperature the dysprosium orders into the same form with the same wave vector; only the cyclic rotation is counter-rotational to that of the iron.<sup>16</sup>

Paixão *et al.*<sup>16</sup> using single-crystal neutron diffraction and Langridge *et al.*<sup>17</sup> using resonant x-ray diffraction found weak superlattice peaks in the ⟨110⟩ directions around Bragg peaks, with a modulation of *nτ*, where *τ*≈0.133 and *n* is odd. These superlattice peaks arise from the long-range cycloidal antiferromagnetic ordering of the iron and the dyspro-

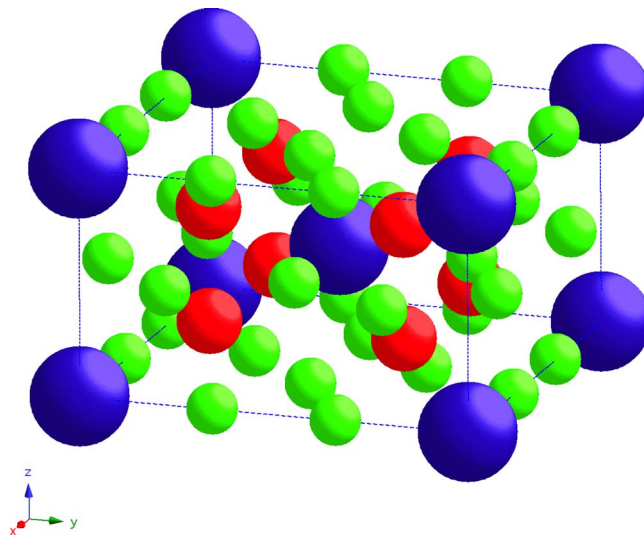


FIG. 1. (Color online) Crystal structure of DyFe<sub>4</sub>Al<sub>8</sub>. The dysprosium (large dark blue) atoms are at the origin and the center of the unit cell in a cage formed by the eight iron (red) atoms. The remaining atomic positions are those of aluminum (small light green).

sium atoms. Paixão *et al.*<sup>16</sup> found the value of  $\tau$  to vary with temperature. Initially, on cooling,  $\tau=0.138$  at  $T_{N(\text{Fe})}$ , and then reducing to  $\tau=0.127$  at  $\sim 80$  K, before increasing again to  $\tau=0.132$  at 2 K.

Neutron studies are extremely sensitive to the magnetic moments on atoms; however, they probe the total magnetic moment, and so it is difficult to determine the individual elemental contributions of the moments. Although in the case of  $\text{DyFe}_4\text{Al}_8$  it was possible using neutron diffraction to separate the dysprosium moment from the overall magnetic moment through symmetry considerations, a direct probe to separate the elemental contribution to the total magnetic moment has, until recently, not been available. Resonant x-ray studies, such as those performed by Langridge *et al.*, observed only  $E1$  electric dipole transitions at the  $L_{2,3}$  edges of Dy, which probe the  $5d$  band. These edges lie at approximately 8 keV and are easily accessible at resonant scattering beamlines. Unfortunately, the magnetic moments on the atoms in the title compound occur in the Fe  $3d$  electron band, and the Dy  $4f$  band, where the corresponding absorption edges lie in the region of 1 keV, energies which until very recently, have not been exploited using diffraction.

New advances in soft x-ray diffraction allow the  $L$  edge of the transition metals<sup>18</sup> and the  $M$  edges of the lanthanides<sup>19</sup> to be reached. The resonant enhancement of the magnetic x-ray scattering is considerably larger at these edges; more importantly these virtual transitions directly probe the electron bands of interest. By tuning to different atomic absorption edges resonant soft x-ray scattering is thus an atomic-selective, band-sensitive, spectroscopic probe of the electronic and magnetic structure. In this paper we demonstrate the use of resonant soft x-ray scattering at the individual atomic absorption edges to separate the individual magnetic ordering of the Dy  $4f$  and Fe  $3d$  electron bands.

Dramatic changes were found in the integrated intensity of the resonant (dipole) features at the Dy  $L_3$  and  $L_2$  edges by Langridge *et al.*<sup>17</sup> This meant that the branching ratio (here defined as the ratio of the integrated intensities of the  $L_3$  to  $L_2$  edges) displayed a highly unusual temperature variation. As we will demonstrate, our experiments, which directly probe the Dy  $4f$  electron band, show no such temperature variation in the  $4f$  band, supporting the theory that the effect observed by Langridge *et al.* occurs only in the  $5d$  band, and appears entirely unconnected to the magnetic state of the system.

## II. EXPERIMENTAL DETAILS AND RESULTS

Experiments were performed on a single crystal of  $\text{DyFe}_4\text{Al}_8$ , grown by the Czochralski method from a levitated melt using high-purity starting materials. The sample was aligned with the  $[110]$  direction surface normal, presenting a highly polished  $1 \times 1 \text{ mm}^2$  sample face to the beam. Previous neutron<sup>16</sup> and x-ray<sup>17</sup> scattering experiments on this sample have shown the existence of superlattice peaks, originating through the ordering of the iron and dysprosium sublattices. The sample was examined at the X1B beamline, NSLS, and the ID08 beamline, ESRF. Both beamlines provide incident x rays with energies in the region of the Dy

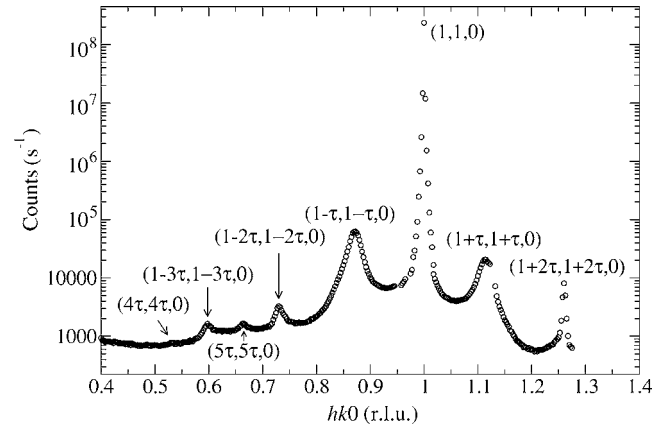


FIG. 2. Superlattice peaks measured at the Dy  $M_5$  edge in the  $[110]$  direction from the origin at 20 K. Data measured at X1B.

$M_{4,5}$  and Fe  $L_{2,3}$  edges. At each beamline the sample was mounted in the center of an in-vacuum diffractometer, and cooled using a liquid helium cold finger allowing a base temperature of 18 K at X1B and 20 K at ID08. The APPLE II undulator x-ray source on the ID08 beamline supplied 100% polarized light, which for this experiment was configured to give a horizontal linear polarized beam, coupled with a vertical scattering geometry. By contrast, the X1B beamline has a 28% vertically polarized beam at 1300 eV, while the scattering geometry was in the horizontal plane. Neither of the beamline chambers possessed the ability to perform postscatter polarization analysis.

Strong x-ray scattering was obtained from the  $(110)$  Bragg peak, which is observable at all energies. The peak intensity was dramatically increased at x-ray energies close to the Dy  $M_5$  edge. Satellite scattering peaks were observed with wave vectors  $(1 \pm n\tau, 1 \pm n\tau, 0)$ , where  $n$  is odd, corresponding to those observed by neutron scattering. In addition we observed peaks where  $n$  was even, these peaks are evident in the  $hk0$  scan shown in Fig. 2, measured at the Dy  $M_5$  edge. This scan in reciprocal space along  $[110]$  corresponds to the high-resolution  $\theta-2\theta$  direction.

High-resolution energy scans at fixed  $Q$  of the Bragg peak,  $(1-\tau, 1-\tau, 0)$  and  $(1-2\tau, 1-2\tau, 0)$  satellite peaks (Fig. 3), were measured on the ID08 beamline, ESRF, at 20 K, with  $\Delta E \approx 50$  meV at 1300 eV. These scans all show a large resonant enhancement at the Dy  $M_5$  edge, and a much weaker enhancement at the  $M_4$  edge. The resonance of the  $(1-\tau, 1-\tau, 0)$  satellite peak at the Dy  $M_5$  edge is split into two strong peaks at 1293 and 1296 eV, with a shoulder on the high-energy side of the latter peak. The Bragg peak shows a similar resonance, but with a weaker resonant enhancement, and a much broader resonance. Proportionally, however, the  $M_4$  edge is stronger, compared to the  $M_5$  edge, on the Bragg peak than the magnetic satellite peak. The splitting at the the  $M_5$  edge is most likely due to the presence of a crystal field splitting in the Dy  $4f$  electron band, lifting the degeneracy. This spectrum of the  $(1-2\tau, 1-2\tau, 0)$  satellite is significantly different from the spectra of either the Bragg peak of the magnetic  $(1-\tau, 1-\tau, 0)$  peak, suggesting a different origin for the  $n$  even and odd satellite peaks.

The resonant x-ray scattering cross section can be written in terms of geometrical factors depending on the incident and

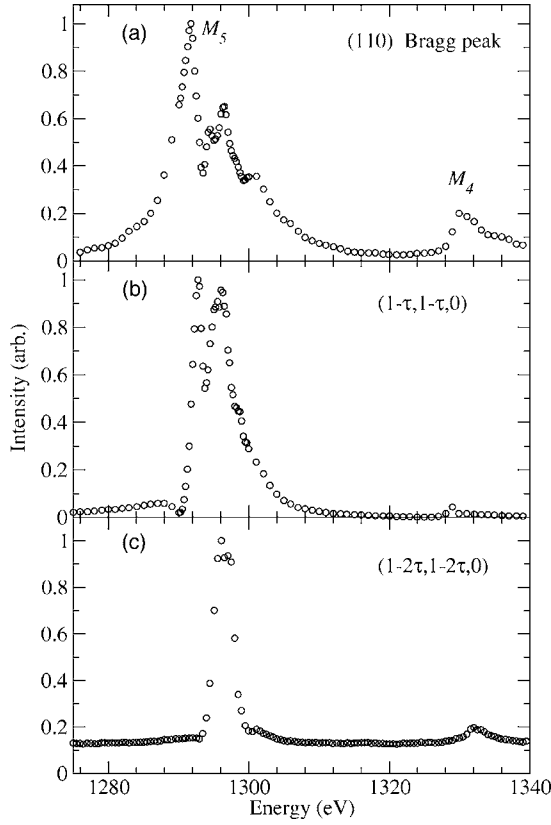


FIG. 3. Scattered x-ray intensity as a function of incident photon energy at the constant wave vector of  $\vec{Q}=(a)$  (110) (b)  $(1-\tau, 1-\tau, 0)$ , and (c)  $(1-2\tau, 1-2\tau, 0)$  through the Dy  $M_4$  and  $M_5$  edges. Data measured at 20 K (ID08).

scattered photons and a tensor characteristic of the scattering ion. For dipole-dipole ( $E1$ ) transitions there are three terms and the scattering amplitude is given as<sup>20</sup>

$$f^{E1} = (\boldsymbol{\epsilon}' \cdot \boldsymbol{\epsilon})F^0 + [(\boldsymbol{\epsilon}' \times \boldsymbol{\epsilon}) \cdot \hat{\mathbf{z}}]F^1 + [\boldsymbol{\epsilon}' \cdot \vec{\mathbf{T}} \cdot \boldsymbol{\epsilon}]F^2, \quad (1)$$

where  $\boldsymbol{\epsilon}$  ( $\boldsymbol{\epsilon}'$ ) are the incident (scattered) x-ray polarization vector and the terms  $F^0$ ,  $F^1$ , and  $F^2$  govern the strength and energy dependence of the resonance and are given by the atomic properties<sup>21</sup>

$$F^{(0)} = (3/4k)[F_{11} + F_{1-1}],$$

$$F^{(1)} = (3/4k)[F_{11} - F_{1-1}],$$

$$F^{(2)} = (3/4k)[2F_{10} - F_{11} - F_{1-1}]. \quad (2)$$

The first term of Eq. (1) is a scalar and represents the resonant enhancement of the Thompson charge scattering and is responsible for the enhancement seen on the (110) Bragg reflection. This term does not result in any rotation of the photon's polarization.

The second term probes a tensor of rank 1 (vector) of odd time reversal symmetry, and results from a net spin polarization of the  $4f$  states, or a difference between overlap integrals, or lifetimes, for the two channels.<sup>21-23</sup> This term re-

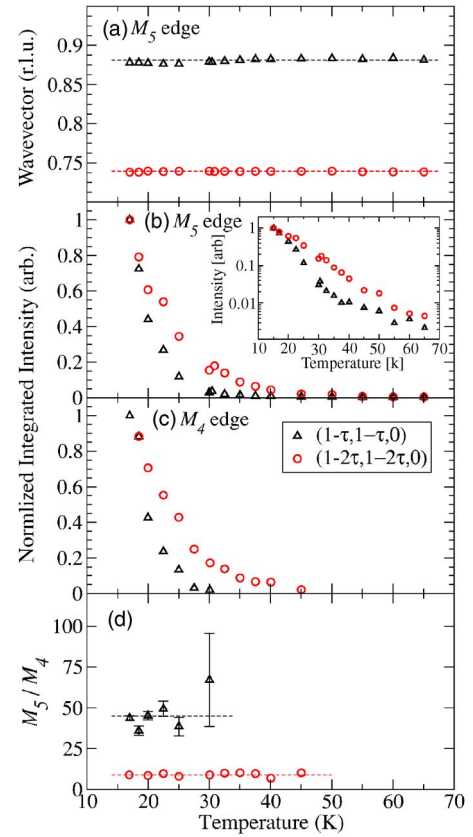


FIG. 4. (Color online) (a) Position and (b) integrated intensity of the  $(1-\tau, 1-\tau, 0)$  and  $(1-2\tau, 1-2\tau, 0)$  superlattice peaks measured at the Dy  $M_5$  edge as a function of temperature. The inset of (b) shows the same plot on a logarithmic scale. This clarifies the existence of a signal up to 65 K. (c) Temperature dependence of the integrated intensity  $(1-\tau, 1-\tau, 0)$  and  $(1-2\tau, 1-2\tau, 0)$  superlattice peaks as measured at the Dy  $M_4$  edge. (d) shows the ratio of the integrated intensity of the superlattice peaks at the  $M_5$  and  $M_4$  edges. Note that the integrated intensities in (b) and (c) are normalized. Data measured at XIB.

sults in a rotation of the photon's polarization. It is this term that is responsible for the magnetic satellite reflections corresponding to  $(\tau, \tau, 0)$ .

The third term probes a tensor of rank 2 and is even in time reversal symmetry. This tensor is invariant under the point group symmetry of the unit cell. This term is taken to be proportional to the electric quadrupole moment; i.e., the asphericity of the atomic charge density. The asphericity may be intrinsic to the lattice (as it is in the case of Templeton scattering<sup>24</sup>) or it can be due to the ordering of electric quadrupole moments. It is this term that is responsible for the second-order satellites observed at  $(2\tau, 2\tau, 0)$ . These satellites have previously been observed in rare earth systems<sup>25</sup> and, due to their appearance at  $2\vec{Q}$  positions, are normally only observable in noncollinear superstructures. This term may rotate the polarization of the photon.

The temperature dependencies of the  $(1-\tau, 1-\tau, 0)$  and  $(1-2\tau, 1-2\tau, 0)$  superlattice peaks at the Dy  $M_{4,5}$  edges were measured at the XIB beamline (Fig. 4). Both superlattice peaks display similar temperature dependences when

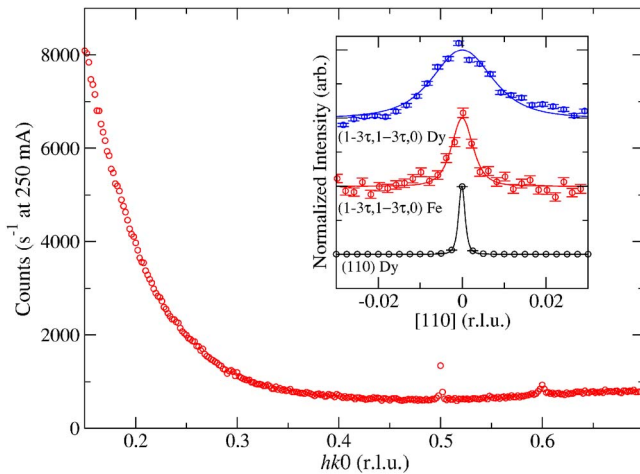


FIG. 5. (Color online) Intensity of the scattered x-ray beam at the Fe  $L_3$  edge along  $[110]$ . The small peak at  $(0.5, 0.5, 0)$  is  $\lambda/2$  leakthrough from the  $(110)$  Bragg peak, while the  $(1-3\tau, 1-3\tau, 0)$  satellite can be seen as the weak peak near  $(0.6, 0.6, 0)$ . The inset plot shows the widths of the  $(1-3\tau, 1-3\tau, 0)$  satellite peaks at both the Fe  $L_3$  edge and Dy  $M_5$  edge. In addition the  $(001)$  Bragg peak at the Dy  $M_5$  edge is shown.

measured at the  $M_5$  edge, and the signal could be detected up to a temperature of 65 K [Fig. 4(b)]. This transition temperature was slightly greater than that detected through other methods, suggesting that soft x-ray diffraction is very sensitive to the dysprosium magnetic moments. The peaks displayed an exponential decrease in intensity with increasing temperature through the temperature range 17–65 K. Measurements were also taken at the Dy  $M_4$  edge [Fig. 4(c)], where the signal from the  $(1-\tau, 1-\tau, 0)$  peak was undetectable above 30 K, while the  $(1-2\tau, 1-2\tau, 0)$  peak was observed up to 45 K.

Many reports, including measurements of magnetic susceptibility by Talik *et al.*,<sup>26</sup> have shown a magnetic transition at 180 K. This has been associated with a magnetic order of the Fe ions. In order to measure this, we conducted resonant scattering with the incident x-ray energy corresponding to the Fe  $L_{2,3}$  edges. This reduced the size of the Ewald sphere, and as such it was not possible to reach much further out in reciprocal space than the  $(1-3\tau, 1-3\tau, 0)$  superlattice peak. A scan in the  $[110]$  direction at the Fe  $L_3$  edge is shown in Fig. 5, where a signal from the  $(1-3\tau, 1-3\tau, 0)$  magnetic peak was seen. There is also a signal at  $(0.5, 0.5, 0)$ , but this originates from  $\lambda/2$  incident wavelength x-rays from the  $(110)$  Bragg peak. It was difficult to observe any satellite peaks at lower  $q$  values as the background scatter increases dramatically. The  $(1-3\tau, 1-3\tau, 0)$  satellite was only observed at the Fe  $L_2$  and  $L_3$  edges (Fig. 6), no signal was seen at the Fe  $L_1$  edge. The resonant spectra of the  $(1-3\tau, 1-3\tau, 0)$  shows a single peak corresponding to the Fe  $L_3$  edge, and a very weak peak at the Fe  $L_2$  edge. Neither peak displayed any fine structure, when measured with an energy resolution of approximately 220 meV (X1B), suggesting a degeneracy of the Fe  $3d$  electron band. As with  $(1-\tau, 1-\tau, 0)$  and  $(1-2\tau, 1-2\tau, 0)$  at the Dy  $M_5$  edge, no large changes were observed in the wave vector of the superlattice

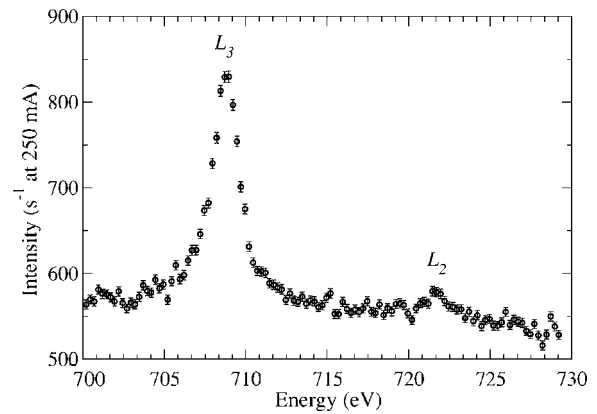


FIG. 6. Scattered x-ray intensity as a function of incident photon energy at the constant wave vector  $\vec{Q}=(1-3\tau, 1-3\tau, 0)$ , measured through the Fe  $L_{2,3}$  edges. No signal was observed at the Fe  $L_1$  edge. The scan was conducted at 17 K at X1B.

peak throughout the temperature range [Fig. 7(a)]. The temperature dependence of the intensity of  $(1-3\tau, 1-3\tau, 0)$  superlattice peak is shown in Fig. 7(b). The intensity of the  $(1-3\tau, 1-3\tau, 0)$  peak at the Fe  $L$  edges was much weaker, even at very low temperatures, than the intensity of the superlattice peaks at the dysprosium absorption edges. This is most likely due to this peak being a harmonic of the magnetic order; unfortunately it is impossible to observe the  $(1-\tau, 1-\tau, 0)$  peak at the Fe  $L$  edges due to Bragg's law. The signal was undetectable above 55 K despite many previous studies showing an ordering in the region of 185 K. The detection of the magnetic signal on the Fe ions corresponds

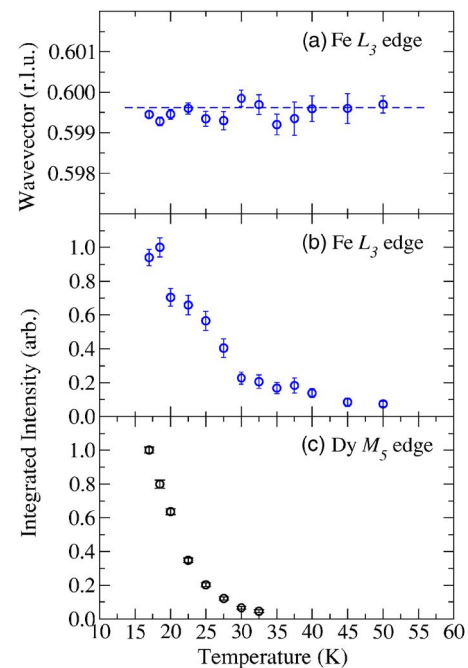


FIG. 7. (Color online) Temperature dependence of the (a) wave vector and (b) intensity of the  $(1-3\tau, 1-3\tau, 0)$  peak at the Fe  $L_3$  edge. The integrated intensity of the  $(1-3\tau, 1-3\tau, 0)$  peak as measured at the Dy  $M_5$  edge as a function of temperature. (c) is shown for comparison. Data measured at X1B.

TABLE I. Full width at half maximum (FWHM) of the main diffraction peaks in reciprocal lattice units of each of the peaks. Notice that the  $(1-\tau, 1-\tau, 0)$  and  $(1-3\tau, 1-3\tau, 0)$  satellite peaks are considerably broader than the  $(1-2\tau, 1-2\tau, 0)$  peak and the  $(1-3\tau, 1-3\tau, 0)$  peak at the Fe  $L_3$  edge.

Peak	Edge	FWHM (r.l.u.)	Correlation length (Å)
(110)	Dy	$1.96 \times 10^{-3}$	4340(20) <sup>a</sup>
$(1-\tau, 1-\tau, 0)$	Dy	$2.61 \times 10^{-2}$	326(4)
$(1-2\tau, 1-2\tau, 0)$	Dy	$1.60 \times 10^{-2}$	535(23)
$(1-3\tau, 1-3\tau, 0)$	Dy	$1.89 \times 10^{-2}$	466(32)
$(1-3\tau, 1-3\tau, 0)$	Fe $L_3$	$6.48 \times 10^{-3}$	1320(150)

<sup>a</sup>The width of the (001) reflects the x-ray penetration depth rather than the crystal quality.

to the ordering temperature of the Dy ions as reported by Paixão *et al.*,<sup>16</sup> suggesting that the rare earth ordering has a significant effect of the moment on the Fe.

Table I compares the widths of the various superlattice peaks, and their calculated correlation lengths. The width of the (110) Bragg peak corresponds to an x-ray penetration depth of 4340(20) Å. This value is consistent with previous results,<sup>18</sup> taking into account the incident energy, suggesting that the Bragg peak resolution is limited through the penetration length rather than by sample quality.

By comparison to the Bragg peak the correlation lengths of the magnetic superlattice peaks were significantly less, in the order of 300–500 Å. This suggests that the magnetic structure has a fairly short-range order, in the region of tens of unit cells. Each of the magnetic peaks at the Dy  $M_5$  edge is approximately the same width; however, the  $(1-3\tau, 1-3\tau, 0)$  peak measured at the Fe  $L_3$  edge is significantly narrower (Fig. 5), pointing to a far more correlated magnetic sublattice on the Fe. These length scales are difficult to compare to previous results; Paixão *et al.*<sup>16</sup> state that the width of the satellite peak is comparable to that of the Bragg peaks; however, their neutron scattering technique has a relatively low angular resolution.

Electron density distortions of the electron orbits could explain the appearance of the  $(1-2\tau, 1-2\tau, 0)$  superlattice peaks, rather than an electric quadrupole moment. Langridge *et al.*,<sup>17</sup> who observed the peaks through x-ray diffraction, suggested that these distortions arise from a magnetoelastic distortion. If such a crystal lattice distortion existed, this signal would be observable from x rays at nonresonant energies. In an attempt to demonstrate this, the sample was mounted on the high-energy x-ray diffraction beamline BW5 at HASYLAB, to observe possible weak charge superlattice reflections. High-energy diffraction is extremely sensitive to small structural distortions, although it is insensitive to magnetic moments. The beamline, with 100 keV incident x-ray energy, was optimized for high flux, in order to observe weak, relatively diffuse superlattice peaks. As such the resolution was not sufficient to measure the Bragg peak widths with sufficient resolution to compare with the soft x-ray results. The sample was aligned and cooled, and despite observing strong Bragg peaks, no superlattice peaks could be

seen. This null result suggests that there is no accompanying structural distortion. This suggests that the  $(1-2\tau, 1-2\tau, 0)$  peak originates purely from an aspherical  $4f$  electron band, and that all of the satellite signals observed through soft x-ray scattering signals are magnetic in origin. The reason for the difference between the spectra arises from the sensitivity to different physical parameters of the odd and even satellite peaks. This is shown by the dependence of  $F^{(0,1,2)}$  to the spherical harmonics [Eq. (2)].

### III. DISCUSSION

The temperature dependence of the superlattice peaks at the iron edge shows a distinctly different behavior from that previously reported. The signal at the dysprosium edge was first observed at 65 K (Fig. 4), and at the iron edge at 55 K (Fig. 7), despite significant previous evidence of an ordering temperature of the Fe, at 180 K, much higher than the rare earth. This suggests that the increased x-ray energy, and the comparative number of electrons in the valence shell, results in a higher sensitivity to the Dy moment.

The earliest powder neutron measurements<sup>12</sup> on DyFe<sub>4</sub>Al<sub>8</sub> found only one magnetic transition at 25 K, which was attributed to ordering of the iron moments into a conical spiral structure. Later studies showed that this transition is in fact due to the ordering of the dysprosium moments. Further measurements of the order temperature for the dysprosium moments at 30 K is provided by temperature-dependent measurements of the ac and dc magnetic susceptibilities of DyFe<sub>4</sub>Al<sub>8</sub> by Talik *et al.*<sup>26</sup> They found the magnetic susceptibilities to have a pronounced peak at 30 K. In addition a thermomagnetic effect was found below 30 K. Partial ordering of the iron sublattice was believed to occur in the temperature region 50–180 K. Later, bulk Mössbauer measurements suggested that the iron atoms order at 180 K. The results presented here suggest that the ordering temperature of the Dy is rather higher than previously suggested, around 65 K, and that this ordering substantially increases the moment on the Fe ions. This is contrary to the result extrapolated by Paixão *et al.*,<sup>16</sup> where it was suggested that the Fe moment did not change significantly with the Dy magnetic ordering. The width of the superlattice signal at the Fe  $L$  edge is significantly greater than at the Dy edge, suggesting that in addition to a higher ordering temperature, at low temperature the magnetic order is significantly more correlated on the Fe than the Dy. Despite the intensity, and therefore magnetic moment, on the Fe increasing below  $T_{Dy}$ , there is no change in the correlation of the signal. Resonant soft x-ray diffraction can detect a relative change in the magnitude of the magnetic moments on the individual atomic species; however, it is unable to provide a quantitative measure of the magnetic moment.

Resonant x-ray scattering studies at the rare earth  $L_{2,3}$  edges probe electronic dipole transitions ( $E1$ ) from the  $2p_{1/2}$  ( $L_2$  edge) and the  $2p_{3/2}$  ( $L_3$  edge) core levels to the empty  $5d$  states. Such techniques are generally only indirectly sensitive to the  $4f$  magnetic ordering. They do, however, give information on the spin polarization of the  $5d$  band which is coupled to the partially filled  $4f$  shell via spin-orbit coupling

and band structure effects. Coupling between the  $4f$  moments is important in stabilizing many complex magnetic structures via the Ruderman-Kittel-Kasuya-Yosida mechanism. Systematic studies by Kim *et al.*<sup>27</sup> of the resonant scattering amplitudes in  $RNi_2Ge_2$  ( $R=Gd, Tb, Dy, Ho, Er, Tm$ ) found that the branching ratio (the ratio of the  $L_3/L_2$  resonant scattering intensities) varied as a function of the rare earth elements. In  $GdNi_2Ge_2$  the ratio was almost unity, then increased to 3.5 in  $DyNi_2Ge_2$  and then to 8.0 in  $ErNi_2Ge_2$ . Such effects are due to increasing spin-orbit coupling and  $4f$  orbital polarization. In nearly all resonant x-ray scattering studies of particular materials, this branching ratio is constant at all temperatures. This is because the electronic band polarization effects are generally insensitive to thermal effects.

Langridge *et al.*<sup>17</sup> found that in  $DyFe_4Al_8$  this branching ratio ( $L_3/L_2$ ) was temperature dependent. Below 40 K the Dy  $L_2$  resonance decreased in intensity as the temperature was lowered to 10 K, whereas the Dy  $L_2$  resonance dramatically increased in intensity between 25 and 10 K. As such, the branching ratio ( $L_3/L_2$ ), was shown to continually change between 40 and 10 K. In all these measurements the resonances were very simple, comprised of a single  $E1$  dipole transition. There was no sign of higher multipole orders such as  $E2$  (electric quadrupole). Langridge *et al.* speculated that the temperature dependence of the branching ratio was caused by changes in the  $5d$  band polarization caused by the increasingly ordered component of the Dy  $4f$  moment and simultaneous magnetoelastic distortions below  $T_{Dy}$ . Our measurements [Fig. 4(d)] show no change in the  $M$  edge branching ratio ( $M_5/M_4$ ) throughout the temperature range. Furthermore, we observe a Dy magnetic order of the  $4f$  electrons at 65 K, so a change in the Dy  $5d$  electron band polarization at 25–40 K is unlikely to be due to this. It is clear that any changes in  $DyFe_4Al_8$  in the spin polarization of the

$5d$  band at 35–40 K are not replicated in the  $4f$  band, and as such not due to the magnetic order of the Dy  $4f$  band.

It was noted by Paixão *et al.*<sup>16</sup> that the modulation vector of the magnetic superlattice changes slightly below  $T_N$ . Although no significant change is obvious in our results [Fig. 4(a)], the magnitude of the change in the wave vector reported by Paixão *et al.* is within the error bars of our measurements.

#### IV. CONCLUSION

The magnetic structure of  $DyFe_4Al_8$  has been studied using resonant soft x-ray diffraction. Superlattice peaks at  $(1 \pm n\tau, 1 \pm n\tau, 0)$  have been observed at the Dy  $M_{4,5}$  edges and Fe  $L_{2,3}$  edges. These have shown temperature dependencies suggesting that the Dy orders at  $T_{Fe} \geq 65$  K. The ordering of the dysprosium appears to significantly increase the magnitude of the moment of the Fe. No change in the branching ratio of the Dy  $M_{4,5}$  edges is seen; however, a splitting in the resonant spectra is observed, suggesting a crystal field splitting of the Dy  $4f$  electron band.

#### ACKNOWLEDGMENTS

T.A.W.B. wishes to thank EPSRC for support. P.D.H. thanks the University of Durham Research Foundation for support. P.D.H. and T.A.W.B. acknowledge travel assistance from EPSRC. The work at Brookhaven National Laboratory is supported by the U.S. Department of Energy, Division of Materials Science and Engineering, under Contract No. DE-AC02-98CH10886. The authors would like to acknowledge the European Synchrotron Radiation Facility for provision of synchrotron radiation facilities. X-ray measurements at X1B, NSLS were supported by the Office of Basic Energy Sciences, U.S. Department of Energy under Grant No. DE-FG02-06ER46285.

\*Electronic address: p.d.hatton@dur.ac.uk

<sup>†</sup>Present address: Synchrotron SOLEIL, 1'Orme des Merisiers, Saint-Aubin BP 48, 91192 Gif-sur-Yvette, France.

<sup>1</sup>M. S. S. Brooks, O. Eriksson, and B. Johansson, *J. Phys.: Condens. Matter* **1**, 5861 (1989).

<sup>2</sup>N. Plugaru, J. Rubín, J. Bartolomé, C. Piquer, and M. Artigas, *Phys. Rev. B* **65**, 134419 (2002).

<sup>3</sup>J. Miguel-Soriano, J. Chaboy, L. M. García, F. Bartolomé, and H. Maruyama, *J. Appl. Phys.* **87**, 5884 (2000).

<sup>4</sup>J. P. Rueff, R. M. Galéra, C. Giorgetti, E. Dartyge, C. Brouder, and M. Alouani, *Phys. Rev. B* **58**, 12271 (1998).

<sup>5</sup>X. C. Kou, R. Grössinger, G. Wiesinger, J. P. Liu, F. R. de Boer, I. Kleinschroth, and H. Kronmüller, *Phys. Rev. B* **51**, 8254 (1995).

<sup>6</sup>M. J. Cooper, E. Zukowski, D. N. Timms, R. Armstrong, F. Itoh, Y. Tanaka, M. Ito, H. Kawata, and R. Bateson, *Phys. Rev. Lett.* **71**, 1095 (1993).

<sup>7</sup>I. Felner and I. Nowik, *J. Phys. Chem. Solids* **39**, 951 (1978).

<sup>8</sup>P. C. M. Gubbens, A. M. van der Kraan, and K. H. J. Buschow, *J. Magn. Magn. Mater.* **27**, 61 (1982).

<sup>9</sup>J. Gal, I. Yaar, E. Arbaboff, H. Etedgi, F. J. Litterst, K. Aggarwal, J. A. Pereda, G. M. Kalvius, G. Will, and W. Schäfer, *Phys. Rev. B* **40**, 745 (1989).

<sup>10</sup>M. Angst, A. Kreyssig, Y. Janssen, J. W. Kim, L. Tan, D. Wermeille, Y. Mozharivskyij, A. Kracher, A. I. Goldman, and P. C. Canfield, *Phys. Rev. B* **72**, 174407 (2005).

<sup>11</sup>N. P. Duong, E. Brück, P. E. Brommer, A. de Visser, F. R. de Boer, and K. H. J. Buschow, *Phys. Rev. B* **65**, 020408(R) (2001).

<sup>12</sup>W. Schäfer and G. Will, *J. Less-Common Met.* **94**, 205 (1983).

<sup>13</sup>I. H. Hagmusa, E. Brück, F. R. de Boer, and K. H. J. Buschow, *J. Alloys Compd.* **298**, 77 (2000).

<sup>14</sup>W. Suski, J. K. A. Gschneider, and L. Eyring, *Handbook on the Physics and Chemistry of Rare Earth* (Elsevier, Amsterdam, 1996), Vol. 22.

<sup>15</sup>K. H. Buschow and A. M. van der Kraan, *J. Phys. F: Met. Phys.* **8**, 921 (1978).

<sup>16</sup>J. A. Paixao, M. Ramos Silva, S. A. Sorensen, B. Lebech, G. H. Lander, P. J. Brown, S. Langridge, E. Talik, and A. P. Gonçalves, *Phys. Rev. B* **61**, 6176 (2000).

- <sup>17</sup>S. Langridge, J. A. Paixao, N. Bernhoeft, C. Vettier, G. H. Lander, D. Gibbs, S. A. Sorensen, A. Stunault, D. Wermeille, and E. Talik, *Phys. Rev. Lett.* **82**, 2187 (1999).
- <sup>18</sup>S. B. Wilkins, P. D. Hatton, M. D. Roper, D. Prabhakaran, and A. T. Boothroyd, *Phys. Rev. Lett.* **90**, 187201 (2003).
- <sup>19</sup>P. D. Spencer, S. B. Wilkins, P. D. Hatton, S. D. Brown, T. P. A. Hase, J. Purton, and D. Fort, *J. Phys. C* **17**, 1725 (2005).
- <sup>20</sup>J. P. Hannon, G. T. Trammell, M. Blume, and D. Gibbs, *Phys. Rev. Lett.* **61**, 1245 (1988).
- <sup>21</sup>J. P. Hill and D. F. McMorrow, *Acta Crystallogr., Sect. A: Found. Crystallogr.* **52**, 236 (1996).
- <sup>22</sup>M. Blume, *J. Appl. Phys.* **57**, 3615 (1985).
- <sup>23</sup>M. Blume and D. Gibbs, *Phys. Rev. B* **37**, 1779 (1988).
- <sup>24</sup>D. Templeton and L. Templeton, *Acta Crystallogr., Sect. A: Found. Crystallogr.* **41**, 133 (1985).
- <sup>25</sup>D. Gibbs, D. R. Harshman, E. D. Isaacs, D. B. McWhan, D. Mills, and C. Vettier, *Phys. Rev. Lett.* **61**, 1241 (1988).
- <sup>26</sup>E. Talik, J. Szade, and J. Heimann, *Physica B* **190**, 361 (1993).
- <sup>27</sup>J. W. Kim, Y. Lee, D. Wermeille, B. Sieve, L. Tan, S. L. Budko, S. Law, P. C. Canfield, B. N. Harmon, and A. I. Goldman, *Phys. Rev. B* **72**, 064403 (2005).